Inorg. Chem. **2003**, *42*, 4738–4742

Nanoscale Pt(0) Particles Prepared in Imidazolium Room Temperature Ionic Liquids: Synthesis from an Organometallic Precursor, Characterization, and Catalytic Properties in Hydrogenation Reactions

Carla W. Scheeren,[†] Giovanna Machado,[†] Jairton Dupont,*[,†] Paulo F. P. Fichtner,[‡] and Sérgio Ribeiro Texeira[§]

Laboratory of Molecular Catalysis, Institute of Chemistry, Department of Metallurgy, and Institute of Physics, UFRGS, Av. Bento Gonçalves, 9500 Porto Alegre 91501-970 RS, Brazil

Received April 29, 2003

The reaction of $Pt_2(dba)_3$ (dba = bis-dibenzylidene acetone) dispersed in room temperature 1-*n*-butyl-3-methylimidazolium (BMI) hexafluorophosphate ionic liquid with molecular hydrogen (4 atm) at 75 °C leads to stable and isolable nanometric Pt(0) particles. The X-ray diffraction analysis (XRD) of the material indicated that it is constituted of Pt(0). Transmission electron microscopy (TEM) analysis of the particles dispersed in the ionic liquid shows the formation of $[Pt(0)]_n$ nanoparticles of 2.0–2.5 nm in diameter. A detailed examination of the nanoparticles imbibed in the ionic liquid and their environment shows an interaction of the BMI·PF_6 ionic liquid with the Pt(0) nanoparticles. The isolated $[Pt(0)]_n$ nanoparticles can be redispersed in the ionic liquid or in acetone or used in solventless conditions for liquid–liquid biphasic, homogeneous, or heterogeneous hydrogenation of alkenes and arenes under mild reaction conditions (75 °C and 4 atm). The recovered platinum nanoparticles can be reused as a solid or redispersed in the ionic liquid several times without any significant loss in catalytic activity.

Introduction

Organic solvents and water "soluble" transition-metal nanoparticles typically of less than 10 nm in diameter are now emerging as an important family of catalysts for various reactions.[1] For example, these redispersible metal nanoparticles in organic solvents or in water form one-phase or two-phase catalytic systems for the hydrogenation of various substrates (olefins, arenes, etc.).[2] The catalytic activity and selectivity of soluble-metal-particle catalysts is usually different from that of classical "homogeneous" or "heterogeneous" catalysts.[3] These metal nanoparticles are usually obtained by the reduction of metal compounds in the presence of stabilizing agents such as surfactants, polymers, poly-oxoanions, etc.[4] It is also known that stable metal nanoparticles with a narrow size distribution can be obtained

* To whom correspondence should be addressed. E-mail: dupont@iq.ufrgs.br. Fax: + 55 5133167304.

† Laboratory of Molecular Catalysis, Institute of Chemistry.

‡ Department of Metallurgy.

§ Institute of Physics.

(1) For recent reviews see: (a) Finke, R. G. *Transition-Metal Nanoclusters*; Feldheim, D. L., Foss, C. A., Jr., Eds.; Marcel Dekker: New York, 2002; Chapter 2, pp 17−54. (b) Roucoux, A.; Schulz, J.; Patin, H. *Chem. Rev.* **2002**, *102*, 3757−3778. (c) Bonnemann, H.; Richards, R. M. *Eur. J. Inorg. Chem.* **2001**, 2455−2480.

(2) See for example: (a) Hornstein, B. J.; Aiken, J. D.; Finke, R. G. *Inorg. Chem.* **2002**, *41*, 1625−1638. (b) Widegren, J. A.; Finke, R. G. *Inorg. Chem.* **2002**, *41*, 1558−1572. (c) Huang, Y. L.; Chen, J. R.; Chen, H.; Li, R. X.; Li, Y. Z.; Min, L. E.; Li, X. J. *J. Mol. Catal. A: Chem.* **2001**, *170*, 143−146. (d) Weddle, K. S.; Aiken, J. D.; Finke, R. G. *J. Am. Chem. Soc.* **1998**, *120*, 5653−5666. (e) Landre, P. D.; Richard, D.; Draye, M.; Gazellot, P.; Lemaire, M. *J. Catal.* **1994**, *147*, 214−222. (f) Nasar, K.; Fache, F.; Lemaire, M.; Beziat, J. C.; Besson, M.; Gallezot, P. *J. Mol. Catal.* **1994**, *87*, 107−115.

(3) Widegren, J. A.; Finke, R. G. *J. Mol. Catal. A: Chem.* **2003**, *191*, 187−207.

(4) See for example: (a) Aiken, J. D.; Finke, R. G. *J. Am. Chem. Soc.* **1998**, *120*, 9545−9554. (b) Weddle, K. S.; Aiken, J. D.; Finke, R. G. *J. Am. Chem. Soc.* **1998**, *120*, 5653−5666. (c) Aiken, J. D.; Finke, R. G. *J. Am. Chem. Soc.* **1999**, *121*, 8803−8810. (d) Aiken, J. D.; Finke, R. G. *Chem. Mater.* **1999**, *11*, 1035−1047. (e) Widegren, J. A.; Weiner, H.; Miller, S. M.; Finke, R. G. *J. Organomet. Chem.* **2000**, *610*, 112−117. (f) Widegren, J. A.; Aiken, J. D.; Ozkar, S.; Finke, R. G. *Chem. Mater.* **2001**, *13*, 312−324. (g) Nagata, T.; Pohl, M.; Weiner, H.; Finke, R. G. *Inorg. Chem.* **1997**, *36*, 1366−1377. (h) Watzky, M. A.; Finke, R. G. *J. Am. Chem. Soc.* **1997**, *119*, 10382−10400. (i) Watzky, M. A.; Finke, R. G. *Chem. Mater.* **1997**, *9*, 3083−3095. (j) Pan, C.; Pelzer, K.; Philippot, K.; Chaudret, B.; Dassenoy, F.; Lecante, P.; Casanove, M. J. *J. Am. Chem. Soc.* **2001**, *123*, 7584−7593. (k) Pellegatta, J.-L.; Blandy, C.; Colliere, V.; Choukron, R.; Chaudret, B.; Cheng, P.; Philippot, K. *J. Mol. Catal. A: Chem.* **2002**, *178*, 55−61. (l) Schulz, J.; Roucoux, A.; Patin, H. *Chem. Eur. J.* **2000**, *6*, 618−624. (m) Schulz, J.; Roucoux, A.; Patin, H. *Chem. Commun.* **1999**, 535−536. (n) Reetz, M. T.; Maase, M. *Adv. Mater.* **1999**, *11*, 773−777. (o) Reetz, M. T.; Winter, M.; Breinbauer, R.; Thurn-Albrecht, T.; Vogel, W. *Chem. Eur. J.* **2001**, *7*, 1084−1094. (p) Reetz, M. T.; Lohmer, G. *Chem. Commun.* **1996**, 1921−1922. (q) Beller, M.; Fischer, H.; Kuhlein, K.; Reisinger, C. P.; Herrmann, W. A. *J. Organomet. Chem.* **1996**, *520*, 257−259. (r) Klingelhofer, S.; Heitz, W.; Greiner, A.; Oestreich, S.; Forster, S.; Antonietti, M. *J. Am. Chem. Soc.* **1997**, *119*, 10116−10120. (s) Chen, C. W.; Akashi, M. *Langmuir* **1997**, *13*, 6465−6472. (t) Bronstein, L. M.; Sidorov, S. N.; Gourkova, A. Y.; Valetsky, P. M.; Hartmann, J.; Breulmann, M.; Colfen, H.; Antonietti, M. *Inorg. Chim. Acta* **1998**, *280*, 348−354.

10.1021/ic034453r CCC: $25.00
Published on Web 06/21/2003

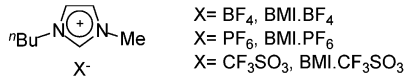

Figure 1. Imidazolium room temperature ionic liquids.

by the decomposition of organometallic precursors in the zero oxidation state using a reactive gas (CO and hydrogen, for instance) under mild reaction conditions. It has hence been, for example, possible to prepare, using polymers as stabilizing agents, stable mono- and bimetallic nanoparticles without contamination of their surfaces.[5]

Our group has recently reported that stable and redispersible transition-metal nanoparticles could be easily obtained by simple reduction, with molecular hydrogen, of transition-metal compounds dissolved in 1-*n*-butyl-3-methylimidazolium hexafluorophosphate (BMI·PF_6, Figure 1) ionic liquid.[6] It has been suggested that the combined intrinsic high charge plus the steric bulk of these salts, which can be described as polymeric supramolecules with weak interactions,[7] can create an electrostatic and steric colloid-type stabilization of transition-metal nanoparticles, similar to the proposed model for the stabilization of nanoclusters by polyoxo-anions or by tetralkylammonium salts.[8] It is therefore of interest to determine whether imidazolium ionic liquids[9] could be used as stabilizing agents for nanoparticles using the decomposition of zerovalent organometallic precursors. This method is also quite interesting since it avoids the use of halogen-containing transition-metal precursors and it will thus be possible to verify if the presence of halogen anions is necessary for the effective stabilization of the nanoparticles prepared in imidazolium ionic liquids.[10]

We describe herein the synthesis and characterization of Pt(0) nanoparticles prepared by simple decomposition of $Pt_2(dba)_3$ in BMI·PF_6 ionic liquid. We also present the catalytic properties of these nanoparticles in the "solventless", homogeneous and two-phase hydrogenation of alkenes and arenes.

Results and Discussion

The submission of a violet "solution" of $Pt_2(dba)_3$ in 1-*n*-butyl-methylimidazolium hexafluorophosphate ionic liquid to 4 bar of hydrogen for 1.5 h afforded a black suspension. Centrifugation of this mixture afforded a black solid that was washed with acetone and dried under reduced pressure. X-ray diffraction analysis clearly identified crystalline Pt(0) in the isolated material (Figure 2). The diffraction lines (111, 200, 220, 311, 222) of metallic Pt can be clearly observed in the diffraction pattern (Figure 2).

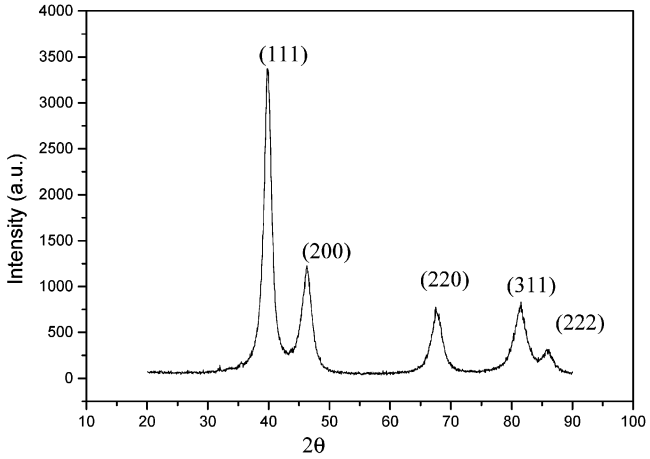

Figure 2. XRD analysis of Pt(0) nanoparticles.

There are a wide variety of techniques for particle or nanoparticle depositions in a suitably dispersed state on a support film for TEM analysis. One of the major requirements for examination is to achieve a good dispersion of the specimen preparation: that is to say, to ensure that a cluster of smaller particles is broken up or at least clearly identifiable as aggregates. The ability to assess the shape as well as the linear dimensions of particles gives electron microscopy an interpretational advantage over indirect methods for measuring the size of particles.[11] It is, of course, important that the distribution of the dispersed particles is not modified by specimen preparation. Inasmuch as most of the 1,3-dialkylimidazolium ionic liquids have extremely low vapor pressure and relatively high viscosity at room temperature (2−4 P),[12] in situ TEM observations in redispersed BMI·PF_6 can in principle be carried out. In this work, the nanoparticles were prepared by two methods: (i) The nanoparticles were mixed with an epoxy resin distributed between two silicon wafer pieces and then dried at 50 °C for 30 min in order to prepare cross section TEM samples. The samples were prethinned mechanically to a thickness of about 20 μm and then ion milled to electron transparency using 3 kV Ar^+ ion beams. (ii) The nanoparticles were dispersed in the BMI·PF_6 ionic liquid and agitated ultrasonically, and then, a droplet was deposited on holey carbon film supported by a copper grid. The grids were placed on filter paper to remove the excess material and allowed to dry out for 2 h under high vacuum. Finally, these TEM samples were

(5) See for example: (a) Rodriguez, A.; Amiens, C.; Chaudret, B.; Casanove, M. J.; Lecante, P.; Bradley, J. S. *Chem. Mater.* **1996**, *8*, 1978−1986. (b) Dassenoy, F.; Philippot, K.; Ould-Ely, T.; Amiens, C.; Lecante, P.; Snoeck, E.; Mosset, A.; Casanove, M. J.; Chaudret, B. *New J. Chem.* **1998**, *22*, 703−711 (c) Pan, C.; Dassenoy, F.; Casanove, M. J.; Philippot, K.; Amiens, C.; Lecante, P.; Mosset, A.; Chaudret, B. *J. Phys. Chem. B* **1999**, *103*, 10098−10101.

(6) Dupont, J.; Fonseca, G. S.; Umpierre, A. P.; Fichtner, P. F. P.; Teixeira, S. R. *J. Am. Chem. Soc.* **2002**, *124*, 4228−4229.

(7) (a) Dupont, J.; Suarez, P. A. Z.; de Souza, R. F.; Burrow, R. A.; Kintzinger, J. P. *Chem. Eur. J.* **2000**, *6*, 2377−2381. (b) Wadhawan, J. D.; Schroder, U.; Neudeck, A.; Wilkins, S. J.; Compton, R. G.; Marken, F.; Consorti, C. S.; de Souza, R. F.; Dupont, J. *J. Eletroanal. Chem.* **2000**, *493*, 75−83. (c) Schroder, U.; Wadhawan, J. D.; Compton, R. G.; Marken, F.; Suarez, P. A. Z.; Consorti, C. S.; de Souza, R. F.; Dupont, J. *New J. Chem.* **2000**, *24*, 1009−1015.

(8) (a) Ozkar, S.; Finke, R. G. *J. Am. Chem. Soc.* **2002**, *124*, 5796−5810. (b) Aiken, J. D.; Finke, R. G. *J. Mol. Catal. A: Chem.* **1999**, *145*, 1−44. (c) Reetz, M. T.; Helbig, W.; Quaiser, S. A.; Stimming, U.; Breuer, N.; Vogel, R. *Science* **1995**, *267*, 367−369.

(9) For a recent review about ionic liquids see: Dupont, J.; de Souza, R. F.; Suarez, P. A. Z. *Chem. Rev.* **2002**, *102*, 3667−3691.

(10) Fonseca, G. S.; Umpierre, A. P.; Dupont, J.; Fichtner, P. F. P.; Teixeira, S. R. *Chem. Eur. J.*, in press.

(11) Niemantsverdriet, J. W. *Spectroscopy in Catalysis*; VCH: Weinheim, 1995.

(12) For the physical−chemical properties of imidazolium ionic liquids see: (a) Suarez, P. A. Z.; Einloft, S.; Dullius, J. E. L.; de Souza, R. F.; Dupont, J. *J. Chim. Phys. Phys.-Chim. Biol.* **1998**, *95*, 1626−1639. (b) Dullius, J. E. L.; Suarez, P. A. Z.; Einloft, S.; de Souza, R. F.; Dupont, J.; Fischer, J.; De Cian, A. *Organometallics* **1998**, *17*, 815−819.

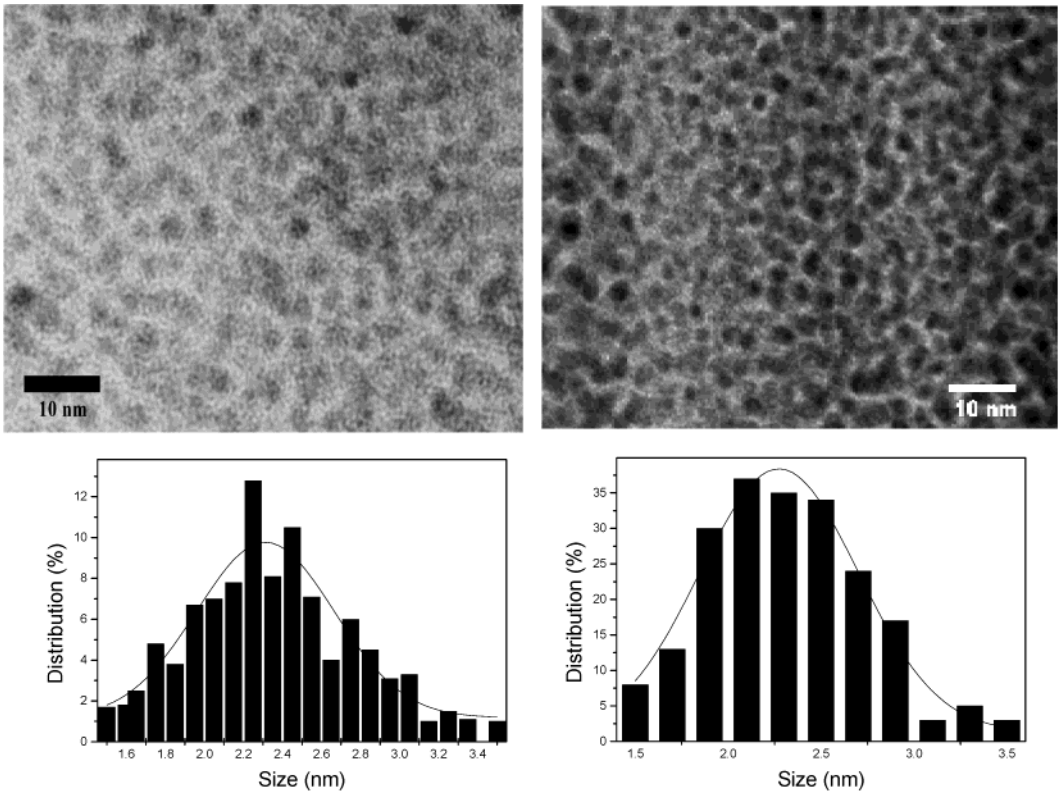

Figure 3. TEM micrographs and histograms showing the particle size distribution of Pt(0) in the epoxy resin (left) and in the BMI·PF_6 ionic liquid (right).

examined using a JEM-2010 microscope operating at an accelerating voltage of 200 kV.

Bright field TEM observations were performed under slight underfocus conditions ($\Delta f \approx -300$ nm) at high magnification (magnification $\geq$ 400 000 times), and particle size distributions were determined once the original negative had been digitalized and expanded to 470 pixels/cm (Figure 3). The particles display an irregular shape, but evaluation of their characteristic diameter results in a monomodal particle size distribution. A mean diameter $d_m \approx 2.5$ nm of the Pt(0) nanoparticles was estimated from ensembles of 200−400 particles found in an arbitrary chosen area of the enlarged micrographs. Figure 3 shows the obtained particle size distributions that can be reasonably well fitted by a Gaussian curve.

A more detailed examination of the nanoparticles imbibed in the ionic liquid and their environment shows a rather strong fluctuation of the contrast density (see Figure 4). Such contrast fluctuations are characteristic of amorphous substrates. The images were compared with those of a pure carbon film as well as with the images from samples containing only ionic liquid droplets under the same imaging conditions.

The presence of the constituent elements of each observation field (i.e., pure carbon, ionic liquid over carbon, and nanoparticles imbibed in the ionic liquid over the carbon film) was checked by EDS measurements. No feature or contrast density could be observed in the pure liquid phase, which has the tendency to form droplets very probably due to its low "ionic-philicity" for the carbon film. On the other hand, it became clear that the contrast fluctuations for the particles imbibed in the ionic liquid and spread over the

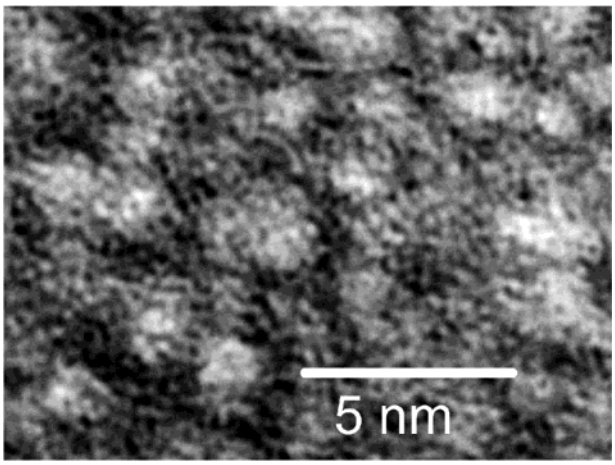

Figure 4. TEM micrograph (negative image, underfocus) of the Pt(0) in BMI·PF_6 ionic liquid showing the contrast density fluctuation around the metal nanoparticles.

carbon are quite distinct from those observed for the pure carbon film as well as for the pure liquid droplets over the carbon film. The sample regions containing particles imbibed in the ionic liquid should not present a high contrast density fluctuation if the surrounding ionic liquid would maintain its liquid features as in the pure liquid observation field. Hence, the high contrast density fluctuation observed in the image shown in Figure 4 reflects the increase of thickness and of mass density of an amorphous structure as if the liquid molecules around the nanoparticles have become immobilized and strongly attached to the nanoparticles. The perimeter and the core of the particle images also show strong contrast density fluctuations under larger underfocus conditions, and with increasing underfocus, it becomes difficult

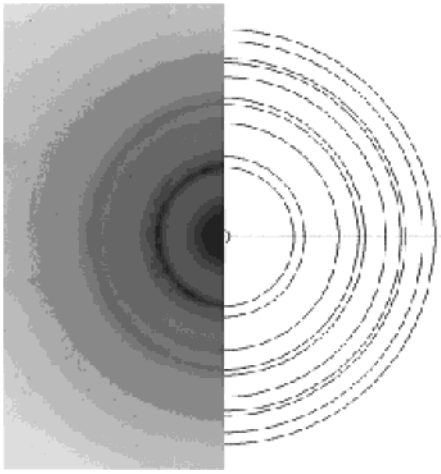

Figure 5. Electron diffraction micrograph obtained by TEM of the Pt particles. Theoretical Pt ring pattern (right side) and experimental (left side).

to discriminate between the individual particles. These observations offer strong evidence of the interaction features of the BMI·PF_6 ionic liquid with the Pt(0) nanoparticles.

It is clear that there are no significant differences in particle diameter and size distribution regardless of whether they have been dispersed via an epoxy resin or prepared in situ (in the ionic liquid). Energy dispersion spectrometry indicates the presence of Pt, and selected area diffraction shows ring patterns which can be fitted to simulation based on Pt(0) parameters (Figure 5).

The diameter and size distribution of these Pt(0) particles are slightly larger than those obtained by decomposition with molecular hydrogen of $Pt_2(dba)_3$ dissolved in organic solvents and in the presence of PVP.[5b]

The catalytic performance of the Pt(0) nanoparticles as a solid, dispersed in acetone and BMI·PF_6, was evaluated in the hydrogenation of alkenes and arenes under solventless, homogeneous, and biphasic conditions (Table 1).[13] The catalytic performance of Pt(0) particles was compared with that of the classical Adam's catalyst (PtO_2) under the same reaction conditions.

It is clear from the data (entries 1−3) that the reactions performed under solventless and homogeneous (acetone) conditions are completed is less time then those performed with the particles dispersed in BMI·PF_6 (compare entries 1−3, and 4, 7, and 8, Table 1). This difference can be attributed to the typical biphasic conditions of the reactions performed in the ionic liquid, which can be a mass-transfer controlled process.[6] The Pt(0) nanoparticles are quite stable and can be re-reused, as solid, or redispersed in BMI·PF_6, several times with a minimal loss in the catalytic activity (Figure 6). As expected, the catalytic activity decreases with the increase in steric bulk on the C═C bond (see entries 1, 6, and 14, Table 1).

It is also evident that the Pt(0) nanoparticles are relatively more active than the classical Adam's catalyst under the same reaction conditions, in particular in solventless conditions (compare entries 6−7 and 11−12, for examples). It is interesting to note that no unsaturated intermediates (cyclohexadienes or cyclohexenes) were detected in the hydrogenation of benzene or toluene even at earlier stages of the reaction.

Moreover, no cyclohexene was detected in the hydrogenation of 1,3-cyclohexadiene, and this process occurs with the

Table 1. Catalytic Performance of Pt(0) Nanoparticles and PtO_2 in Solventless, Homogeneous, and Biphasic Conditions[a]

entry	medium	catalyst	substrate	product	t (h)	cv (%)[b]	TOF (h^{-1})[c]
1	solventless	$[Pt(0)]_n$	hex-1-ene	hexane	0.25	100	1000
2	acetone	$[Pt(0)]_n$	hex-1-ene	hexane	0.25	100	1000
3	BMI·PF_6	$[Pt(0)]_n$	hex-1-ene	hexane	0.4	100	625
4	BMI·PF_6	$[Pt(0)]_n$	cyclohexene	cyclohexane	1.6	100	156
5	BMI·PF_6	PtO_2	cyclohexene	cyclohexane	1.8	100	138
6	solventless	$[Pt(0)]_n$	cyclohexene	cyclohexane	0.3	100	833
7	solventless	PtO_2	cyclohexene	cyclohexane	1.0	100	250
8	acetone	$[Pt(0)]_n$	cyclohexene	cyclohexane	0.3	100	833
9	BMI·PF_6	$[Pt(0)]_n$	benzene	cyclohexane	10	46	11
10	BMI·PF_6	PtO_2	benzene	cyclohexane	19	93	12
11	solventless	$[Pt(0)]_n$	benzene	cyclohexane	9	100	28
12	solventless	PtO_2	benzene	cyclohexane	10	9	2
13	solventless	$[Pt(0)]_n$	toluene	methylcyclo-hexane	12	83	17
14	BMI·PF_6	$[Pt(0)]_n$	2,3-dimethyl-1-butene	2,3-dimethyl-butane	3	82	68
15	solventless	$[Pt(0)]_n$	2,3-dimethyl-1-butene	2,3-dimethyl-butane	0.6	100	417
16	solventless	$[Pt(0)]_n$	1,3-cyclo-hexadiene	cyclohexane	0.3	100	833

[a] Reaction conditions: [substrate]/[Pt] = 250 at 75 °C and under 4 atm of hydrogen (constant pressure). [b] Substrate conversion. [c] [mol product]/[mol Pt] [hour].

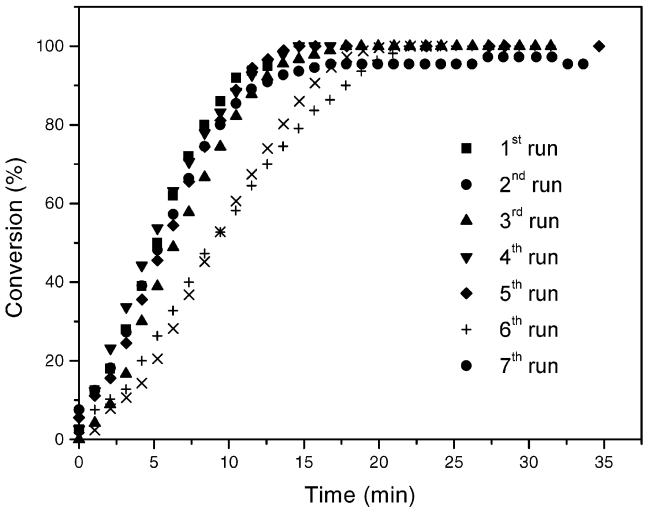

Figure 6. Conversion curves of hex-1-ene hydrogenation by Pt(0) nanoparticles "solventless" at 4 atm and 75 °C, [alkene]/[Pt] = 250, showing the catalyst recycle.

(13) For hydrogenation reactions promoted by transition-metal complexes in imidazolium ionic liquids see: (a) Jessop, P. G.; Stanley, R. R.; Brown, R. A.; Eckert, C. A.; Liotta, C. L.; Ngo, T. T.; Pollet, P. *Green Chem.* **2003**, *5*, 123−128. (b) Navarro, J.; Sagi, M.; Sola, E.; Lahoz, F. J.; Dobrinovitch, I. T.; Katho, A.; Joo, F.; Oro, L. A. *Adv. Synth. Catal.* **2003**, *345*, 280−288. (c) Boxwell, C. J.; Dyson, P. J.; Ellis, D. J.; Welton, T. *J. Am. Chem. Soc.* **2002**, *124*, 9334−9335. (d) Dyson, P. J. *Appl. Organomet. Chem.* **2002**, *16*, 495−500. (e) Brown, R. A.; Pollet, P.; McKoon, E.; Eckert, C. A.; Liotta, C. L.; Jessop, P. G. *J. Am. Chem. Soc.* **2001**, *123*, 1254−1255. (f) Guernik, S.; Wolfson, A.; Herskowitz, M.; Greenspoon, N.; Geresh, S. *Chem. Commun.* **2001**, 2314−2315. (g) Berger, A.; de Souza, R. F.; Delgado, M. R.; Dupont, J. *Tetrahedron: Asymmetry* **2001**, *12*, 1825−1828. (h) Dupont, J.; Suarez, P. A. Z.; Umpierre, A. P.; de Souza, R. F. *Catal. Lett.* **2001**, *73*, 211−213. (i) Dyson, P. J.; Ellis, D. J.; Welton, T. *Can. J. Chem.* **2001**, *79*, 705−708. (j) Steines, S.; Wasserscheid, P.; Driessen-Holscher, B. *J. Prakt. Chem.* **2000**, *342*, 348−354. (k) Monteiro, A. L.; Zinn, F. K.; deSouza, R. F.; Dupont, J. *Tetrahedron: Asymmetry* **1997**, *8*, 177−179. (l) Suarez, P. A. Z.; Dullius, J. E. L.; Einloft, S.; deSouza, R. F.; Dupont, J. *Inorg. Chim. Acta* **1997**, *255*, 207−209. (m) Chauvin, Y.; Mussmann, L.; Olivier, H. *Angew. Chem., Int. Ed. Engl.* **1996**, *34*, 2698−2700.

same TOF at 100% conversion as for cyclohexene (see entries 6 and 16, Table 1). These results are clear indications that the Pt(0) nanoparticles prepared in BMI·PF_6 cannot be used for the selective hydrogenation of dienes to monoenes in opposition to platinum salts immobilized in Et_4SnCl_3 molten salt which are highly selective catalysts for these reactions.[14]

In summary, we have shown that stable Pt(0) nanoparticles of 2−3 nm diameter and with a narrow size distribution can be easily obtained via decomposition of Pt(0) organometallic precursors. TEM analysis of the nanoparticles dispersed in BMI·PF_6 shows for the first time evidence of the interaction of the ionic liquid with the particle surface. These nanoparticles are recyclable catalytic systems for the solventless or biphasic hydrogenation of alkenes and arenes under mild reaction conditions. The catalytic activity of the Pt nanoparticles is higher than that obtained for the classical PtO_2 catalyst under the same reaction conditions.

Experimental Section

General Methods. All reactions involving platinum compounds were carried out under an argon atmosphere in oven dried Schlenk tubes. $Pt_2(dba)_3$ was prepared according to literature procedures.[15] The BMI·PF_6 ionic liquid was prepared according to a known procedure[16] and dried over molecular sieves (4 Å), and its purity was checked by a $AgNO_3$ test, ^1H and ^{31}P NMR, and cyclic voltametry. The water (<0.1 wt %)[17] and chloride[18] (<1.4 mg/L) content in BMI·PF_6 used were determined by known methods. Solvents, alkenes, and arenes were dried with the appropriate drying agents and distilled under argon prior to use. All the other chemicals were purchased from commercial sources and used without further purification. NMR spectra were recorded on a Varian Inova 300 spectrometer. Infrared spectra were performed on a Bomem B-102 spectrometer. Mass spectra were obtained using a GC/MS Shimadzu QP-5050 (EI, 70 eV). Gas chromatography analyses were performed with a Hewlett-Packard-5890 gas chromatograph with an FID and a 30 m capillary column with a dimethylpolysiloxane stationary phase. The X-ray diffraction analysis was performed in a Philips X'Pert MRD diffractometer in a Bragg−Brentano geometry using curved graphite crystal as monochromator. Transmission electron microscopy (TEM) was performed on a JEOL 2010 microscope operating at 200 kV. The TEM images were obtained in bright-field conditions using a 20 μm objective aperture and with the objective lens slightly underfocused ($\Delta f \approx -300$ nm).

The nanoparticle formation and hydrogenation reactions were carried out in a modified Fischer−Porter bottle immersed in a silicone oil bath and connected to a hydrogen tank. The fall in the hydrogen pressure in the tank was monitored with a pressure transducer interfaced through a Novus converter to a PC and the data workup via Microcal Origin 5.0. The temperature was maintained at 75 °C by a hot-stirring plate connected to a digital controller (ETS-D4 IKA). A deliberated stirring of 1200 rpm was used (no ionic catalytic solution projection was observed). The catalyst/substrate ratio was calculated from the initial quantity of $Pt_2(dba)_3$ used.

Nanoparticles Formation and Isolation. In a typical experiment, to a Fischer−Porter bottle containing BMI·PF_6 (1 mL) was added $Pt_2(dba)_3$ (30 mg, 0.02 mmol), which was stirred at room temperature for 15 min resulting in a violet dispersion. The system was heated to 75 °C and hydrogen (4 bar) was admitted to the system. After stirring for 1.5 h, a black "solution" was obtained. The Pt nanoparticles were isolated by centrifugation (3500 rpm) for 3 min and washed with acetone (3 × 15 mL) and dichloromethane (3 × 15 mL) and dried under reduced pressure. The Pt samples thus obtained were prepared for TEM and X-ray analysis, and for catalytic experiments (see in a following paragraph).

Hydrogenations. Liquid−Liquid Biphasic. The arene was added to the ionic catalytic solution obtained as described, and hydrogen was admitted to the system at a constant pressure (see Table 1). Samples for GC and GC-MS analysis were also taken at regular intervals under H_2. The reaction mixture forms a typical two-phase system (lower phase containing the Pt nanoparticles in the ionic liquid and upper phase containing the organic products). The organic phase was separated by decantation or distillation, weighed, and analyzed by GC, GC-MS, and ^1H NMR.

Solventless. The isolated Pt nanoparticles were placed in a Fischer−Porter bottle, and the arene was added. The reactor was placed in an oil bath at 75 °C, and hydrogen was admitted to the system at a constant pressure (4 atm). Samples for GC and GC-MS analysis were also taken at regular intervals under H_2. The organic products were recovered by simple filtration and analyzed by GC.

Homogeneous. The isolated Pt nanoparticles were dispersed in acetone (3 mL) and placed in a Fischer−Porter bottle, and the arene was added. The reactor was placed in an oil bath at 75 °C, and hydrogen was admitted to the system at constant pressure (4 atm). Samples for GC and GC-MS analysis were also taken at regular intervals under H_2. The organic products were recovered by simple filtration and analyzed by GC.

Sample Preparation and TEM Analysis. The samples were prepared according to the following methods: (a) BMI·PF_6 suspension of the Pt nanoparticles was deposited on a holey carbon film fixed within a copper grid. (b) The nanoparticles were mixed with an epoxy resin distributed between two silicon wafer pieces at 50 °C for 30 min. Cross section TEM samples were prethinned mechanically. The thinning to electron transparency was obtained by ion milling. Particle size distributions were determined once the original negative had been digitalized and expanded to 470 pixels/cm for a more accurate resolution and measurement. Typically, TEM pictures of each sample were taken at multiple random locations in the sample and at two different magnifications. The size distribution histogram was obtained on the basis of measurement of around 400 particles.

Sample Preparation and X-ray Analysis. The Pt powder was mixed with vacuum grease and fixed on a glass substrate. A flat surface was obtained by pressing the mixed powder between two flat glasses. The diffraction pattern was obtained after subtraction of the powder spectrum from a background measured using a glass substrate plus the vacuum grease.

Acknowledgment. Thanks are due to CTPETRO-CNPq and FAPERGS for partial financial support. We also thank CAPES for a fellowship to C.W.S.

IC034453R

(14) Parschall, G. W. *J. Am. Chem. Soc.* **1972**, *94*, 8716−8719.
(15) Moseley, K.; Maitlis, P. M. *J. Chem. Soc., Chem. Commun.* **1971**, 982−983.
(16) (a) Suarez, P. A. Z.; Dullius, J. E. L.; Einloft, S.; deSouza, R. F.; Dupont, J. *Polyhedron* **1996**, *15*, 1217−1219. (b) Dupont, J.; Suarez, P. A. Z.; Consorti, C. S.; de Souza, R. F. *Org. Synth.* **2002**, *79*, 236−243.
(17) Sweeny, B. K.; Peters, D. G. *Electrochem. Commun.* **2001**, *3*, 712−715.
(18) Gallo, V.; Mastrorilli, P.; Nobile, C. F.; Romanazzi, G.; Suranna, G. P. *J. Chem. Soc., Dalton Trans.* **2002**, 4339−4342.